Korean J. Chem. Eng., 34(10), 2559-2569 (2017)
DOI: 10.1007/s11814-017-0185-z
pISSN: 0256-1115
eISSN: 1975-7220

REVIEW PAPER

Separation of oil from oily wastewater using low cost ceramic membrane

Bipul Das*,†, Bandana Chakrabarty, and Pranab Barkakati***

*Chemical Engineering Division, CSIR-North East Institute of Science and Technology, Jorhat, Assam, India
**Chemical Engineering Department, Assam Engineering College, Guwahati, Assam, India
(*Received 17 March 2017 • accepted 2 July 2017*)

Abstract−Safe disposal of oily wastewater is a global issue across the industrial world. Stable oil-in-water emulsion has been separated by dead end filtration using low cost ceramic membrane. The efficiency of separation at different oil-water emulsion concentrations was evaluated at different trans-membrane pressures. Maximum rejection of oil 95.4% was observed for membrane sintered at 850 °C for oil concentration of 250 mg/L at 137.89 kPa. The permeate oil concentration was within the permissible range of environmental tolerance (<12 mg/L). The flux decline data was compared with various pore blocking models and it was appraised that cake filtration model best represents the fouling mechanism within the experimental range of pressure and oil-in-water concentration. Solvent permeation studies revealed that nonpolar solvents were more permeable than the polar solvents. The selection parameter of 14.78×10^{-6} $m^3/m^2\cdot s$ indicates a good combination of flux permeation, declination and rejection for the membrane sintered at 900 °C.

Keywords: Low Cost Ceramic Membrane, Oily Wastewater, Oil-water-emulsion, Micro-filtration

INTRODUCTION

With rapid industrial development, enormous quantities of oily wastewater are generated that are not safe for free discharge to the soil and water system in the environment. The hydrocarbon concentration in oily wastewater from various industries like oil & gas, petroleum refineries, pharmaceutical, metallurgical, fertilizers and petrochemicals, usually ranges between 50-1,000 mg/L [1-4]. This concentration is considered hazardous and needs treatment with reduction to a tolerable limit of 10-15 mg/L before being discharged to the environment safely [5-8].

Various methods are being adopted for treatment of oily wastewater in petrochemical as well as other industries releasing oily wastewater, such as ultrasonic separation, coagulation/flocculation, air floatation, chemical de-emulsification and gravity settling [9-12]. But these methods are found to have certain drawbacks in terms of high cost, large space requirement and generation of secondary pollutants (disposal of which has become an additional concern) [13,14]; so at present they are no more considered as effective measures in mitigating the wastewater problem. Rather environmentally benign, energy efficient and cost effective membrane separation processes are gaining popularity as emerging technological solutions for wastewater as well as other applications like catalytic membrane reactors, fuel cells for energy etc. [15-22]. Performance of a membrane is usually measured by its permeability and selectivity. Due to higher selectivity, considerable permeation rate, superior chemical and thermal stability and, most importantly, longer lifetime, ceramic membranes are always preferred to polymeric membranes for industrial application [23-26]. Along with these properties, a good ceramic membrane should also have narrow pore size distribution and low manufacturing cost [27]. All these parameters mainly depend on the raw materials selected, sintering temperature chosen and the method of fabrication of the membrane.

Many researchers have synthesized alumina-based ceramic membranes, but higher cost of raw materials and high sintering temperature are a hindrance to their economic industrial application [28,29]. Therefore, clay based low cost ceramic membranes are gaining attraction as replacement of costly raw materials for industrial purposes in recent times. Many researchers have used low cost clays for fabrication of ceramic membranes such as raw clay, Moroccan clay, Tunisian clay, sepiolite clay, Algerian clay, dolomite and kaolin [30-37]. Kaolin is one of the cheapest and easily available raw materials in India. In the present study kaolin based ceramic membranes prepared by paste casting method [38] were used for the experimental work.

In most of the studies for treatment of oily wastewater using polymeric as well as ceramic membranes, ultra-filtration and microfiltration techniques were focused. Researchers have used low cost and conventional ceramic membranes for the treatment of oil-water emulsions [39-42]. Using kaolin as a raw material, Mohammadi et al. [4] synthesized a tubular ceramic membrane in microfiltration range of pore size 10 μm. They experimented their prepared membrane for treatment of oil-water emulsion at different operating conditions such as applied pressure, cross flow velocity and different oil concentration. They observed that the permeate flux is linearly increased with applied pressure and temperature but inversely proportional to oil concentration. Yang et al. [43] developed a ceramic membrane by using raw material of ZrO_2/α-Al_2O_3 with pore size 0.2 μm and applied it for separation of oil-water emulsions where they attained 99.8% of oil rejection. Considering α-Al_2O_3 as the raw material, Abadi et al. [44] prepared a tubular ceramic membrane of pore size 0.2 μm. They studied for separation of organic carbon

†To whom correspondence should be addressed.
E-mail: bipuldas@neist.res.in, bipul.das27@gmail.com

Table 1. Properties of membranes used for dead-end filtration

Membrane	Sintering temperature (°C)	r_{av} (μm)	Porosity (ε) (%)	PWF ($m^3m^{-2}s^{-1}$)×10^{-6} at 137.89 kPa	CF at 413.68 kPa
M_1	850	0.79	18.88	10.19	0.90
M_2	900	0.91	9.00	33.97	0.85
M_3	950	1.28	5.59	62.16	0.80

PWF: pure water flux; CF: compaction factor

by varying different parameters like trans-membrane pressure, cross flow velocity and temperature. They recorded more than 95% total organic carbon removal and produced permeate with oil and grease concentration of 4 mg/L. Vasanth et al. [45] separated oil-water emulsions using kaolin based ceramic microfiltration membranes with nominal pore size of 1.30 μm and obtained 85-99% oil rejection. They observed inverse relation between oil rejection and applied pressure and direct proportionality between the rejection and oil concentration. Monash et al. [46] investigated the performance of kaolin based ceramic membranes for treatment of oil-in-water emulsion using an oil concentration of 200 mg/L and observed maximum rejection of 99%. Nandi et al. [47] studied the separation of oil-water-emulsion at an oil concentration range of 125-250 mg/L by varying trans-membrane pressure differences and exhibited an oil rejection of 98.8% at 68.9 kPa with an initial oil concentration of 250 mg/L. From applicability perspectives, development of ceramic membranes using mixed clays for oil-water separation is gaining more attention owing to their low cost. The present research focuses the use of kaolin based low cost ceramic membranes for separation of stable oil-water emulsions in the dead-end mode microfiltration.

Low cost ceramic membranes fabricated as per details in our previous work [38] on the basis of their sintering temperature and composition of raw materials were used in dead-end microfiltration experiments to evaluate the membrane performances for flux permeation and oil rejection. The objective of this study was to observe the effect of four distinct trans-membrane pressures at various oil concentrations on rejection of oil and identify the most suitable membrane as per the evaluated selection parameters. The permeability of the fabricated membrane was also examined with various polar and non-polar solvents. From the experimental flux decline records, we analyzed the fouling mechanism.

MATERIALS AND METHODS

1. Raw Materials

Ceramic membranes were prepared using various inorganic raw materials such as kaolin (Otto Chemie, India), quartz (Research-Lab Fine Chem Industries, India), feldspar (National Chemicals, India), activated carbon (Rankem, India), boric acid (Process Chemicals, India), sodium metasilicate (Nice, India) and titanium dioxide (Lobachemie, India). Crude oil sample was collected from the northeastern oil field in Assam. Water used for this work was collected from Q-3 UV (Millipore, France).

2. Preparation and Characterization of Ceramic Membranes

Ceramic membranes were prepared by using the inorganic raw materials in paste casting route. The raw materials in definite ratios were mixed and ground in a mixture grinder (Bajaj GX8, India) followed by paste preparation in pestle mortar with water. The prepared paste was then allowed to set over a gypsum surface using an SS316 ring of 40 mm ID and allowed to cure for 24 hours under a pressure of 2 kg maintaining the homogeneity in the matrix. The fabricated membranes were then dried and sintered at 850, 900 and 950 °C under controlled heating and cooling rates. The details of the composition of raw materials and the procedure of preparation were reported in our previous work [38]. The membranes were designated as M_1, M_2 and M_3 and their properties are presented in Table 1.

The membranes were characterized for identification of their morphological and structural parameters through pure water permeation studies and various analytical techniques. The prepared membrane cost was estimated at 92 \$/m^2 based on the raw materials price, which is more inexpensive than the alumina membrane (cost around \$500/m^2), and it can be considered low cost in the microfiltration range for industrial applications. The details of membrane characterization techniques and cost analysis of the membrane are reported in our previous report [38].

3. Preparation of Stable Oil-in-water Emulsion for Microfiltration Experiments

The microfiltration experiments were at four different concentrations of oil, 100, 150, 200 and 250 mg/L, which were prepared at our laboratory using a mixer homogenizer (Omni International, MX 21209, USA) at 7,000 rpm and 40 °C for 15 minutes. All emulsions of the solution were stable with respect to the nature of coalescence and homogeneity. The oil-water emulsion was considered stable based on the absence of oil layer on the top of the surface for a period of one week. During this period the droplet size distribution, oil concentration and pH of the solution were found to be constant, and all experiments were carried out within this period for avoiding any experimental error. The feed and permeate oil concentrations were determined by using a UV-vis spectrophotometer (PerkinElmer, Lambda 35, USA) at a wavelength of 240 nm, where the maximum absorbance was obtained. The oil droplet size distributions of the feed solution having different concentration are presented in Fig. 1. The oil droplet diameters for various oil concentrations are shown in Table 2.

4. Dead-end Microfiltration Experiment

A schematic of the set-up for separation of oil from the prepared oily water under dead-end mode is shown in Fig. 2. The membrane cell (ID: 40 mm, OD: 70 mm, capacity: 150 ml) was made of Teflon with a flat circular base plate (100 mm dia). The prepared membrane was sealed with epoxy resin (Mseal, Pidilite Industries Ltd., Mumbai, India) after keeping inside the Teflon casing. The Teflon

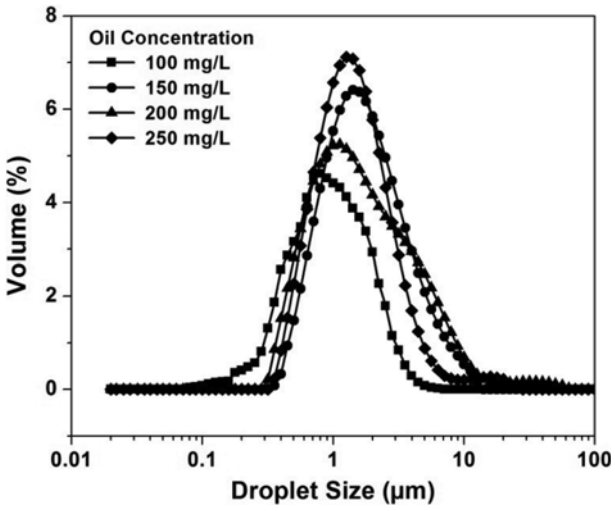

Fig. 1. Droplet size distribution of oil-water emulsions.

Table 2. Properties of oily wastewater used for dead-end filtration

Oil concentration (mg/L)	pH	Density (kg m^{-3})	Droplet size (μm)
100	8.12	998.6	0.08-4.00
150	8.12	997.9	0.76-4.78
200	8.12	996.5	0.61-5.97
250	8.12	993.5	0.68-3.50

casing was then put in the membrane housing of 40 mm diameters on the base plate. After sealing, the permeable diameter and effective permeable area of the membrane were 2.5×10^{-2} m and 4.91×10^{-4} m^2, respectively. During the experiments, 125 ml of feed solution was fed from the top by using a peristaltic pump (Watson Marlow Ltd., 313S, England). The cell was then subjected to pressure in the experimental pressure range (137.89-344.73 kPa) by using nitrogen gas, and the resultant liquid permeate flux was measured by means of a digital scale weighing machine (Kern & Sohn Gmbh, 572-32, Germany) till steady state was achieved after ~40 mins. To remove any loose particles that may be present in the pores, every membrane is compacted by using de-ionized water at a trans-membrane pressure of 413.68 kPa, which is higher than the maximum operating pressure for the conducted experiments. The pure water flux, which was high initially, was observed to decrease gradually with time, and after about three hours of operation became almost steady, indicating the membrane to be ready for the experiment. This compacted membrane was considered for carrying out all the separation experiments. The performance of the membranes was examined for different oil concentrations and different trans-membrane pressures. All permeation experiments were conducted at room temperature.

5. Separation of Oil from Oil-in-water Emulsion

The dead-end MF experiments were carried out to observe the effect of trans-membrane pressure difference and feed oil concentration on the permeate flux in batch mode operations. For each applied pressure and oil concentration of feed solution in the experiments, 10 ml of the initial permeate was discarded and subsequently the volume of permeate was measured in regular interval one minute each.

The permeate flux (J) was calculated by the following equation:

$$J = \frac{V}{At} \tag{1}$$

where V is the permeate volume, A is the effective permeable area and t is permeate time.

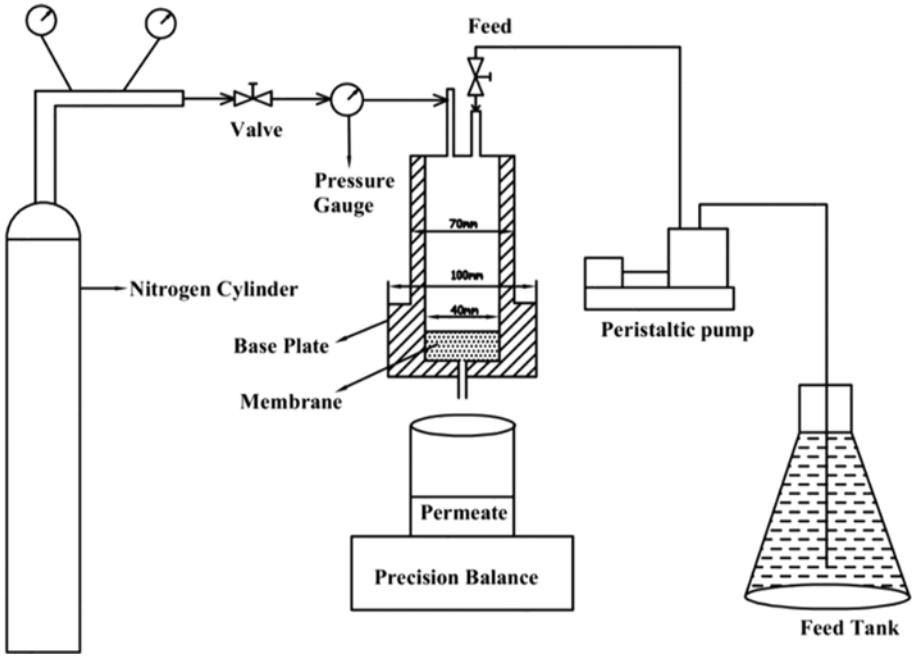

Fig. 2. Dead-end experimental setup for separation study.

Table 3. Physical properties of pure water and solvents for permeation experiment

Solvent	Molecular weight (g/mol)	Density (g/ml)	Viscosity (cP)	Surface tension (mN/m)	Purity (%)
Deionised water	18.01	0.998	1.02	72.00	-
Methanol	32.04	0.792	0.59	22.60	99.00
Ethanol	46.04	0.790	1.20	21.55	99.50
Acetone	58.08	0.791	0.31	24.32	99.00
1-Propanol	60.09	0.803	1.96	23.70	99.50
1-Butanol	74.12	0.810	2.57	24.20	99.00
Pentane	72.15	0.626	0.24	15.48	99.00
Hexane	86.17	0.655	0.32	18.43	99.00
Heptane	100.21	0.684	0.37	20.14	99.00
Toluene	92.14	0.867	0.56	28.52	99.00

The rejection (R) was estimated by using the following equation:

$$R(\%)=\frac{C_f-C_p}{C_f}\times 100 \quad (2)$$

where C_f is feed oil concentration and C_p is the permeate oil concentration.

The oil concentration in feed and permeate samples was evaluated by using a UV-vis spectrophotometer (PerkinElmer, Lambda 35, USA) at a wave length of 240 nm [7]. During the experiment, the oil droplet were deposited over the membrane surface as well as inside the membrane pores which results in flux declination. Flux declination is an indication of membrane fouling.

The flux decline (FD) at any time, t, was evaluated by using the following relation:

$$FD_t(\%)=\frac{J_{pi}-J_{pt}}{J_{pi}}\times 100 \quad (3)$$

where J_{pi} is the starting permeate flux ($m^3m^{-2}s^{-1}$) and J_{pt} is the permeate flux at time t.

The performance of the membranes was measured based on a selection parameter (SP) $m^3m^{-2}s^{-1}$ which is defined as follows:

$$SP=\frac{PF\times R}{FD} \quad (4)$$

where PF=Permeate flux, FD=Flux declination and R=Rejection.

Higher SP value indicates higher flux, higher rejection with a lower range of fouling.

The membranes were cleaned after every experiment to recover the permeability. After each experiment the membranes were washed in tap water continuously for 5 minutes for removing the loose oil particles present in the surface. The membranes were then kept in a sonicator (Sonics & Materials Inc., VCX500, USA) at 20 kHz for 30 mins so that the oil particles would come out from top and inside surface of the membrane due to vibration. Finally, 100 ml of 0.02 N NaOH solution was allowed to pass through the membrane at a pressure of 137.89 kPa for removing the residual oil droplets from the pores. With this cleaning procedure, the membranes were found to regain up to 98% of pure water flux in comparison to the fresh membrane.

6. Solvent Permeation Study

The permeation experiments with various solvents were carried out with the selected membrane based on selection parameter (SP) so as to check its permeability and resistance against those solvents. The physical properties of the solvents used are given in Table 3. Both polar and non-polar solvents of analytical grade were selected to perform the experiments. Methanol, ethanol, propanol, and butanol were chosen as polar solvents and acetone, toluene, pentane, hexane and heptanes were selected as nonpolar solvents for carrying out the permeation studies. Before each experiment, each membrane was cleaned and flushed with the new solvent to remove any probable residual matter left from the previous experiment. Solvent flux was measured as a function of applied pressure, which was in the range of 137.89-344.74 kPa.

FOULING MECHANISM STUDIES

One of the major problems with membranes used for industrial application is the declination of flux with respect to time, which is attributed to fouling mechanism. A number of works have been reported so far on analysis of membrane fouling based on filtration laws. For dead end-filtration at constant pressure, Hermia 1982 [48] identified four major empirical models: complete pore blocking, standard pore blocking, intermediate pore blocking, and cake filtration. All the four pore blocking models are expressed in linear form [49]:

Complete pore blocking $$\ln(J^{-1})=\ln(J_0^{-0.5})+k_bt \quad (5)$$

Standard pore blocking $$J^{-0.5}=J_0^{-0.5}+k_st \quad (6)$$

Intermediate pore blocking $$J^{-1}+J_0^{-1}+k_it \quad (7)$$

Cake filtration $$J^{-2}=J_0^{-2}+k_ct \quad (8)$$

In terms of complete pore blocking, the solute particle size is greater than the membrane pore size and hence reduces the flux by settling the solutes on the top of membrane surface. The solute particle size is considered smaller in comparison to pore size of membrane in case of standard pore blocking. Therefore, the solute particles are deposited inside the membrane pores and reduce the membrane pore volume. In intermediate pore blocking, the solute particle size is equal to the membrane pore. Therefore, in this pore blocking mechanism the solutes are assumed to settle on each other leading to blockage of membrane pores and declination of

permeate flux. On the other hand, the solute particle size is greater than the average pore size of the membrane in cake filtration model. As a result the solute particles settle on the top surface of the membrane and form a cake. This adds to the existing membrane hydraulic resistance, which in turn affects the flux adversely. Amongst the four models, the best fitted model was identified as the one having the maximum value of correlation coefficient (R^2) obtained as a result of fitting the experimental data by linear regression technique.

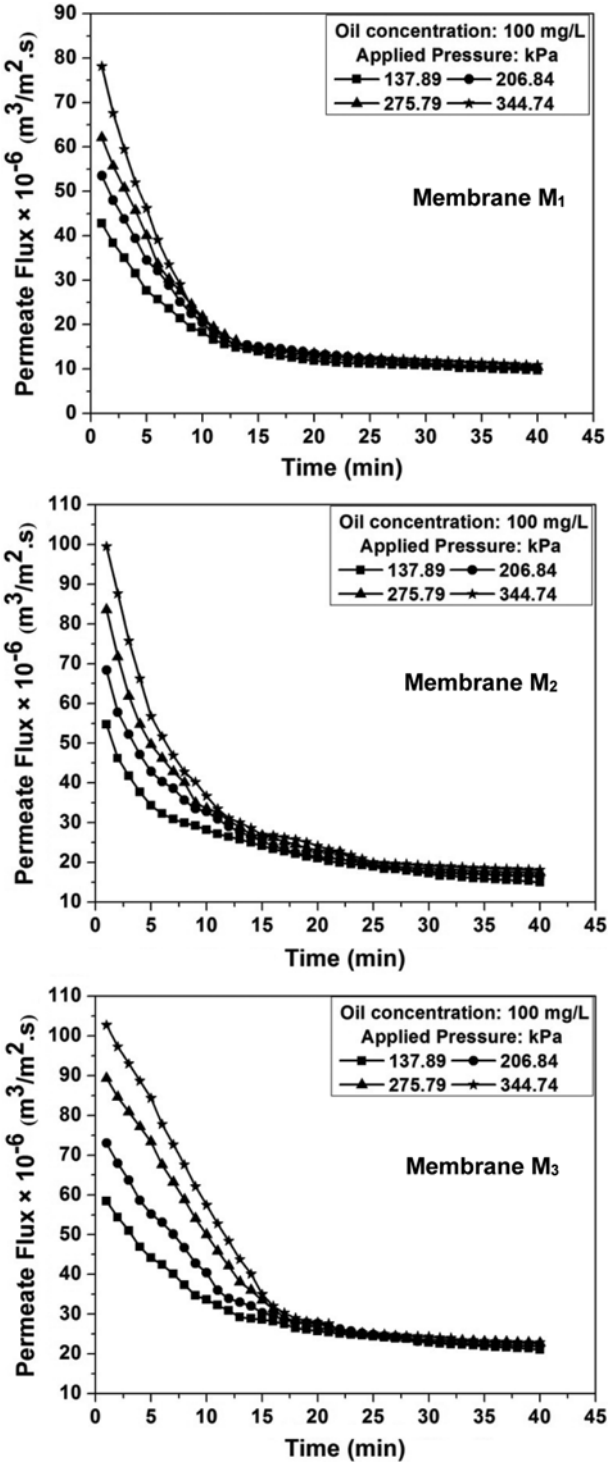

Fig. 3. Variation of permeate flux with time for the membranes at various oil concentrations and trans-membrane pressure of 137.89 kPa.

RESULTS AND DISCUSSION

1. Microfiltration of Oil-water Emulsions

The performance of the three prepared membranes was measured in terms of the permeate flux, the percent rejection and flux declination for different operating conditions. For this the effect of four trans-membrane pressures, 137.89 kPa, 206.84 kPa, 275.79 kPa and 344.74 kPa, and four different oil concentrations, 100 mg/L, 150 mg/L, 200 mg/L and 250 mg/L, were considered.

1-1. Effect of Trans-membrane Pressure

1-1-1. Permeate Flux

Fig. 3 illustrates the effect of trans-membrane pressure on permeate flux for the three prepared membranes (M_1, M_2, M_3) at oil concentration range of 100-250 mg/L. For all the membranes, the permeate flux declined sharply during the initial period of about 10 mins and then gradually became steady. The declination of permeate flux with time may be attributed to the combined effects of pore blocking by the oil droplets as well as concentration polarization on the membrane surface. The permeate fluxes after 40 minutes are noted at the four selected trans-membrane pressures at a fixed oil concentration of 100 mg/L and are shown in Fig. 4 and Fig. 5 for all the three membranes. One observation from these figures is that the permeate flux increased with increase in trans-membrane pressure for all the membranes due to increase in driving force across the membrane. Another observation is that the permeate flux is always found to be higher with M_3 membrane, which is followed by M_2 and M_1, respectively. This is due to the difference in pore size range of the membranes owing to different sintering temperature while preparing the membranes. Similar observations were also reported for dead-end mode of membrane filtration by other researchers [50].

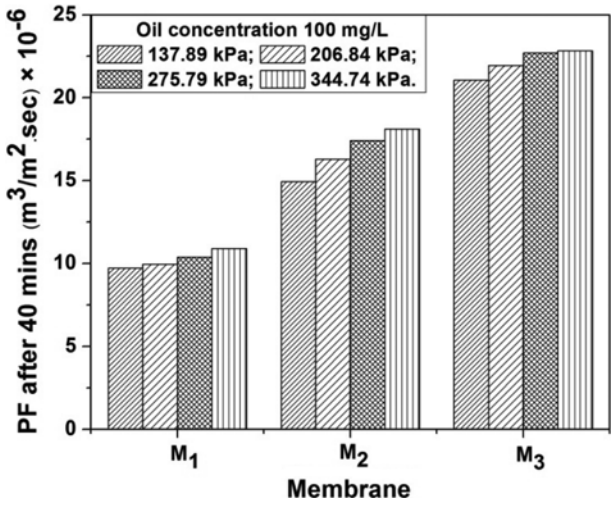

Fig. 4. Permeate flux (PF) of membranes at varying trans-membrane pressures at oil concentration of 100 mg/L after 40 min.

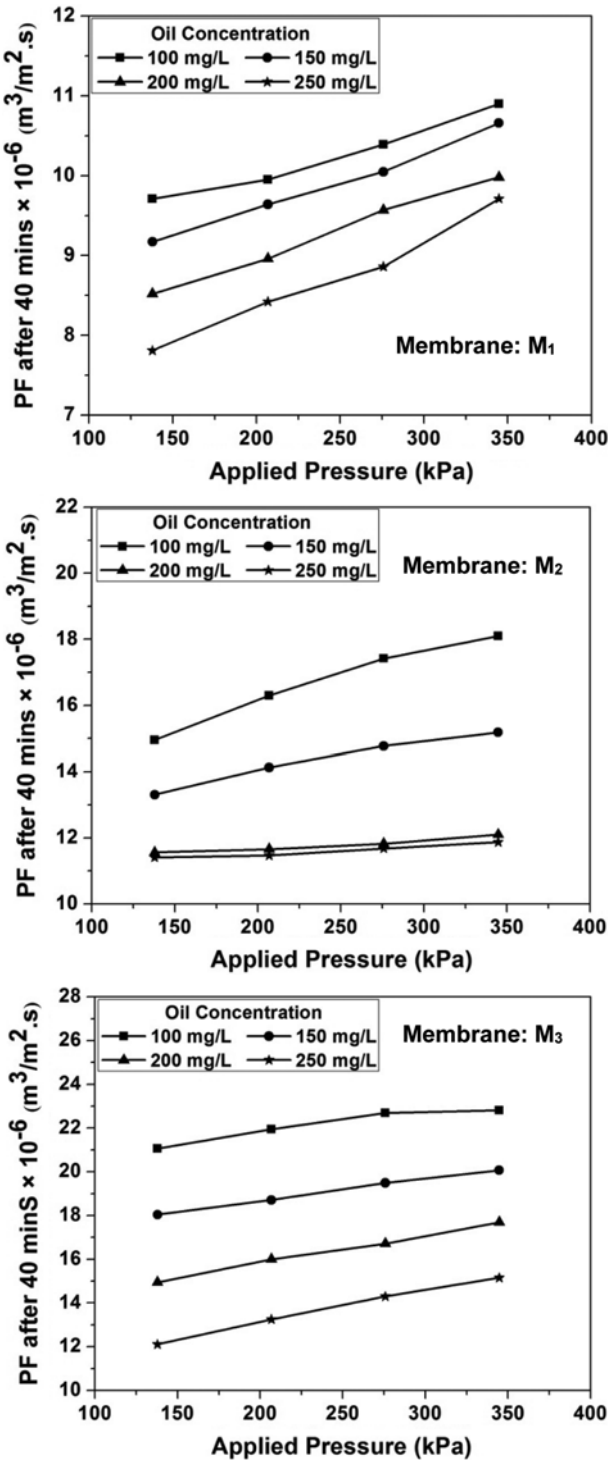

Fig. 5. Effect of trans-membrane pressure on permeates flux at various oil concentrations after 40 mins of permeate time.

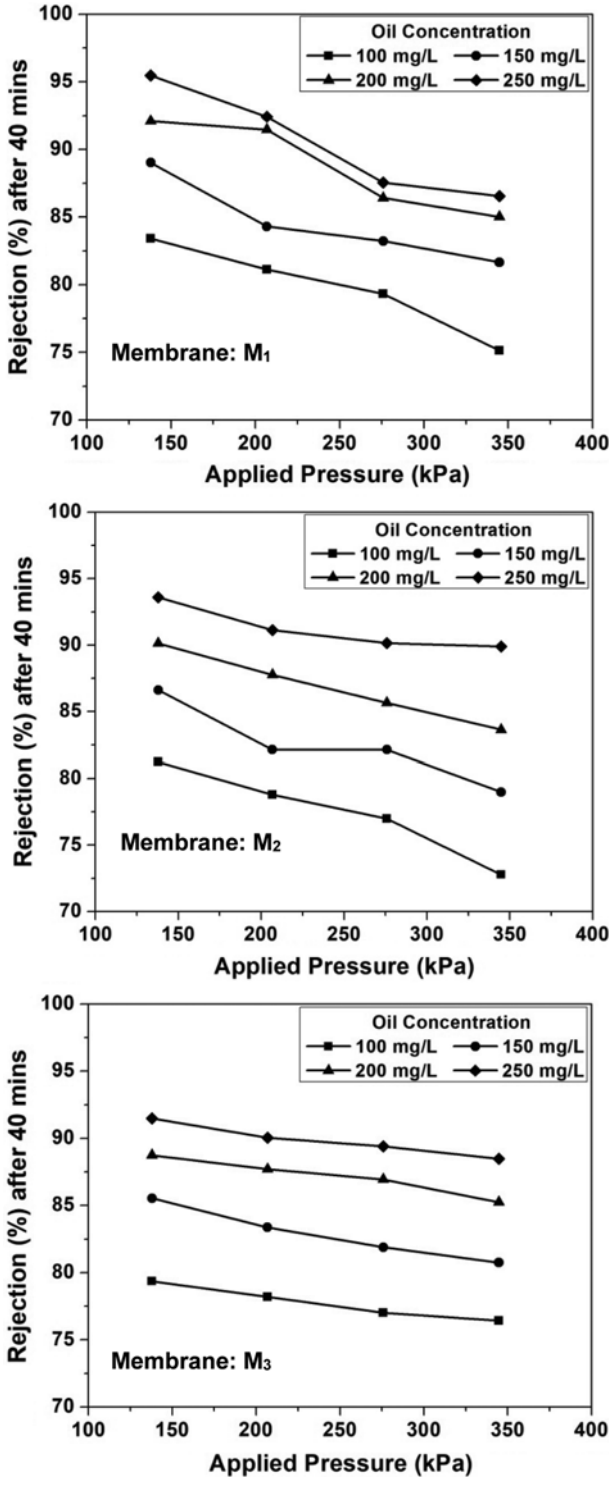

Fig. 6. Effect of the trans-membrane pressure on rejection of oil at various oil concentrations.

1-1-2. Oil Rejection

The effect of the trans-membrane pressure on rejection of oil (%R) from the oily water at different oil concentrations is shown in Fig. 6. In all the experiments, the rejection of oil was recorded in the range of 76 to 95.4% for the selected pressure range. It was observed that pressure in the lower range had higher rejection of oil. Also, with increase in applied pressure the rejection decreased for all the membranes. At higher pressure, the oil droplets may deform and pass through the small pores resulting in decreased rejection. The rejection of oil (%R) at different applied pressures for different oil concentrations is also represented in Table 4. Among the three membranes, the M_1 membrane was found to have highest rejec-

Table 4. Rejection (%) of oil for membranes (M_1, M_2 and M_3) at different oil concentrations and various trans-membrane pressures

Applied pressure (kPa)	Feed oil concentration (mg/L)											
	100	150	200	250	100	150	200	250	100	150	200	250
	Rejection (%) Membrane M_1				Rejection (%) Membrane M_2				Rejection (%) Membrane M_3			
137.89	83.42	89.02	92.09	95.47	81.23	86.61	90.12	93.59	78.36	85.53	88.74	91.48
206.84	81.12	84.30	91.46	92.42	78.78	82.14	87.76	91.12	78.19	83.37	87.70	90.04
275.79	79.32	83.22	86.41	87.55	76.98	82.14	85.65	90.14	77.02	81.88	86.94	89.39
344.74	75.12	81.66	85.01	86.54	72.78	78.98	83.63	89.89	76.42	80.74	85.24	88.47

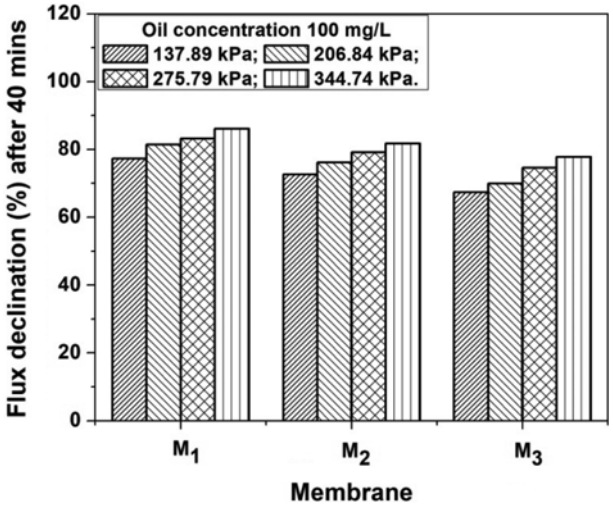

Fig. 7. Effect of trans-membrane pressure on flux declination (%) for different membranes at different trans-membrane pressure and fixed oil concentration of 100 mg/L after 40 mins permeate time.

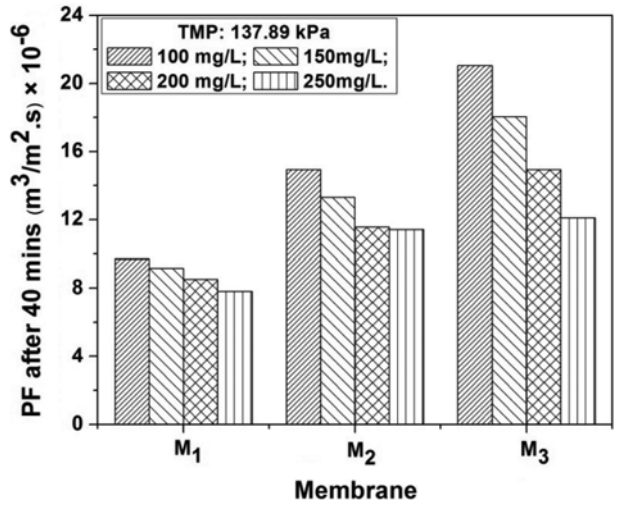

Fig. 8. Effect of oil concentration on permeates flux (PF) at trans-membrane pressure: 137.89 kPa of the membranes.

tion ability at all the oil concentrations and trans-membrane pressures considered. The maximum rejection of 95.4% was obtained at an applied pressure of 137.89 kPa for an oil concentration of 250 mg/L with the M_1 membrane.

1-1-3. Flux Declination

Flux declination with time is an important factor for evaluation of performance of any membrane, as it may be considered an indication of fouling tendency of a particular membrane. From Fig. 3, for any trans-membrane pressure, the flux declines with time and after a period of about 30-40 minutes, the flux becomes steady. The variation of % flux declination (calculated by Eq. (3)) of the three membranes with varying trans-membrane pressure at a fixed oil concentration of 100 mg/L is shown in Fig. 7. The % flux declination increased with increase in trans-membrane. The increase in flux declination with pressure was due to concentration polarization and pore blocking of oil droplets. With increasing pressure, the interaction between oil droplets increased and hence coalescence of the oil-water emulsions led to formation of larger oil droplets. As a result, an oily layer was formed on the membrane surface, causing membrane fouling at a greater rate. Fig. 7 also compares the performance of the three membranes in terms of their fouling tendencies. The M_1 membrane has the highest tendency of fouling.

1-2. Effect of Oil Concentration

1-2-1. Permeate Flux

The effect on permeate flux with different feed oil concentrations (i.e. 100, 150, 200 and 250 mg/L) at different trans-membrane pressures is shown in Fig. 5. It is observed that with increasing oil concentration the permeate flux decreased at a particular trans-membrane pressure for each membrane. With increasing oil concentration, the viscosity increased, which in turn reduced the flow rate. In addition, the rejected oily layer that formed on the membrane surface provides resistance to the permeate flux. Fig. 8 illustrates that permeate flux calculated after 40 minutes with respect to different oil concentrations at a trans-membrane pressure of 137.89 kPa for the three membranes. All the membranes have shown the same trend, i.e., decrease of flux with increase in oil concentration. Also, the M_3 membrane gave the highest flux, irrespective of any oil concentrations compared to the other two membranes.

1-2-2. Oil Rejection

Rejection of oil with respect to different oil concentrations is shown in Fig. 6 and Fig. 9. The details of the rejection data with respect to different oil concentrations and types of membranes are in Table 4. Clearly, the rejection of oil increased with increasing concentration of oil in the feed for all the selected membranes. This may be due to the increase in the oil droplet density and size. Higher concentration of the oil led to coalescence of the oil drop-

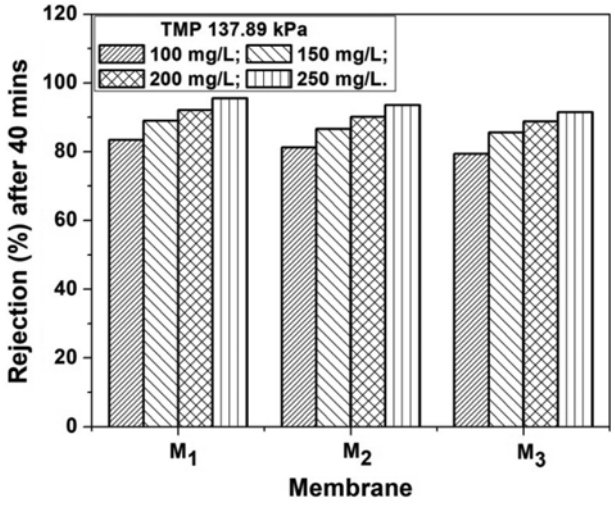

Fig. 9. Effect on oil rejection (%R) at different oil concentration and at constant trans-membrane pressure of 137.89 kPa.

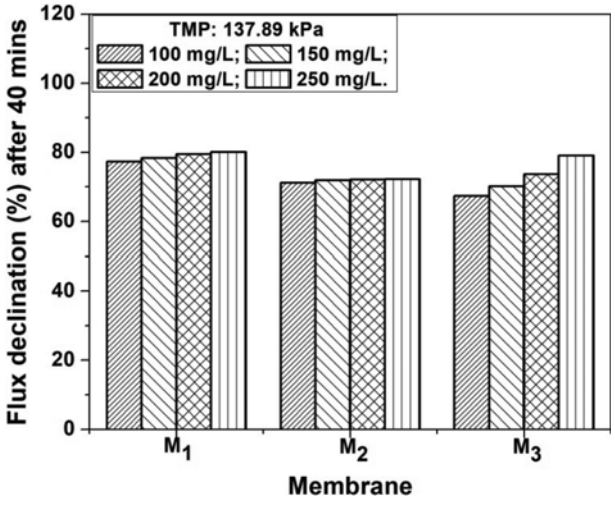

Fig. 10. Effect of oil concentration on flux declination (%) for different membranes at trans-membrane pressure of 137.89 kPa after 40 mins permeates time.

lets to form bigger droplets that eventually resulted in higher rejections. In all the experiments the rejections were recorded in the range of 76 to 95%. The maximum rejection of 95.4% was obtained at an applied pressure of 137.89 kPa for an oil concentration of 250 mg/L in the M_1 membrane.

1-2-3. Flux Declination

Fig. 10 illustrates the variation of flux declination with oil concentration at a trans-membrane pressure of 137.89 kPa for the three membranes. The highest flux declination is experiential with the high concentration of oil at 250 mg/L for all the membranes. With greater concentration of oil, the fouling of membrane becomes quicker because of possible increase in occurrence of concentration polarization and pore blocking due to coalescence of oil droplets. The flux declination of the M_1 membrane is higher compared to M_2 and M_3 membranes, which indicates that lower pore size membrane has higher intensity of fouling. Another observation is that the variation in flux declination with oil concentration is more significant in M_2 and M_3 membranes compared to M_1 membrane. This may be attributed to difference in the morphology of the membranes.

Table 5. Flux declination (% FD) of different membrane at trans-membrane pressure of 137.89 kPa

Membranes	Flux declination (%) after 40 mins at 137.89 kPa			
	100 mg/L	150 mg/L	200 mg/L	250 mg/L
M_1	77.30	78.32	79.43	80.11
M_2	72.67	72.98	75.58	77.19
M_3	67.34	70.19	73.65	79.00

1-3. Optimization of Membrane

The performance of the membranes was analyzed in terms of the selection parameter (SP) (calculated by Eq. (4)), which includes permeate flux, rejection and flux declination at an oil concentration of 250 mg/L and trans-membrane pressure of 137.89 kPa. The details of the findings are in Table 6. Each membrane has showed different results. From the table, M_2 has the highest SP value with 14.78×10^{-6} $m^3/m^2\cdot s$, which is followed by M_3 (with SP of 14.02×10^{-6} $m^3/m^2\cdot s$) and M_1 (with SP of 9.31×10^{-6} $m^3/m^2\cdot s$), respectively. So, based on this, the M_2 membrane may be recommended for separation of oil at the selected operating conditions (137.89 kPa pressure and 250 mg/L oil concentration).

2. Solvent Permeation Experiment

Fig. 11 shows that the relation between the solvent flux and trans-membrane pressure is linear; this implies that trans-membrane pressure is the only driving force which determines the solvent permeation through the membrane. Fig. 12 indicates that non-polar solvents exhibit better permeability than the polar solvents. This may be ascribed to the hydrophobic nature of the prepared membranes. It is also observed that the permeability of methanol and pentane are approximately two times higher than that of ethanol and heptane. Apart from the applied pressure, viscosity also plays an important role on the solvent permeability. Fig. 13 represents a correlation between the solvent permeability and the inverse of the

Table 6. Selection parameters of membranes at 137.89 kPa and 250 mg/L feed oil concentration

Membranes	PF $(m^3m^{-2}s^{-1})\times10^{-6}$	R (%)	FD (%)	SP $(m^3m^{-2}s^{-1})\times10^{-6}$
M_1	7.81	95.47	80.11	9.31
M_2	11.41	93.59	72.24	14.78
M_3	12.11	91.48	79.00	14.02

PF: permeate flux; R: rejection; FD: declination of flux; SP: selection parameter

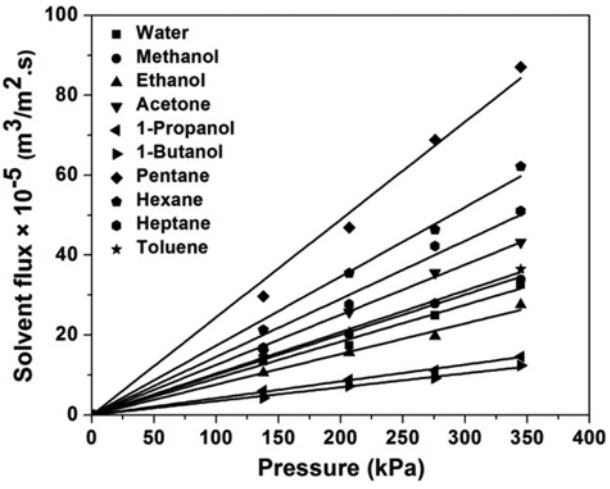

Fig. 11. Solvent flux of the membrane M_2 at different trans-membrane pressure.

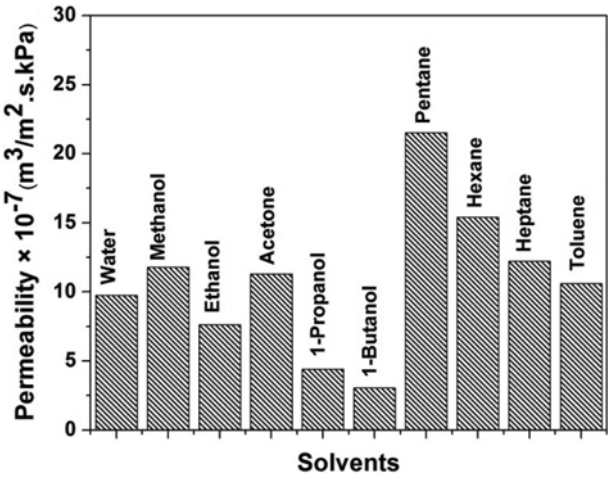

Fig. 12. Solvent permeability of various solvents of membrane M_2 at various trans-membrane pressure.

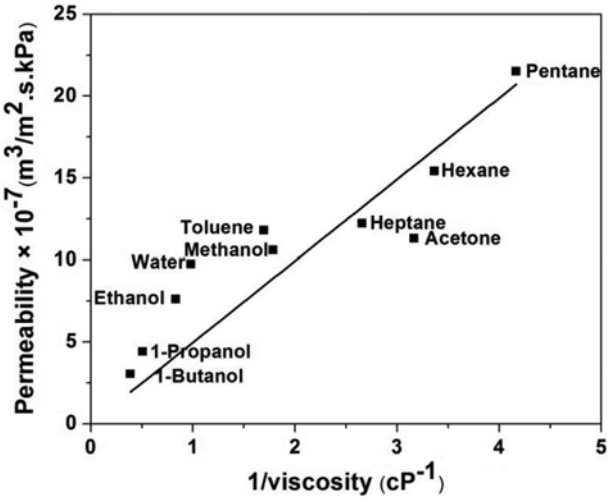

Fig. 13. Variation of solvent permeability with viscosity of membrane M_2 for various solvents.

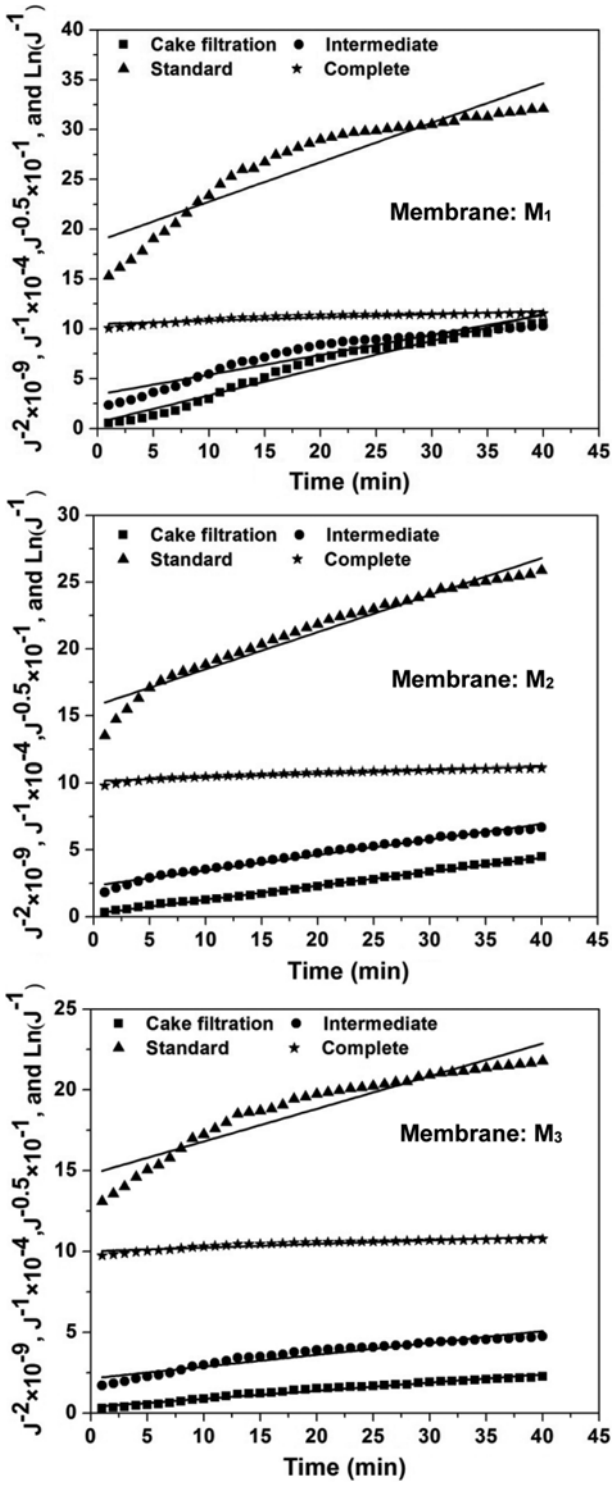

Fig. 14. Permeate flux vs. time for different pore blocking models at trans-membrane pressure of 137.89 kPa.

solvent viscosity. For solvent of identical groups the permeability increases with decreases in solvent viscosity. Also observed is that the flux of acetone is smaller than that of hexane. With viscosity as controlling factor for the solvent, acetone flux should have been more than that of hexane. This implies that in addition to viscosity, the solvent surface tension also plays a role in the solvent per-

Table 7. Parameters for various pore blocking models

Membrane type	Complete pore blocking			Standard pore blocking			Intermediate pore blocking			Cake filtration		
	k_b	$\ln(J_o^{-1})$	R^2	k_s	$J_o^{-0.5}\times10^{-1}$	R^2	k_i	$J_o^{-1}\times10^{-4}$	R^2	k_c	$J_o^{-2}\times10^{-9}$	R^2
M_1	0.032	10.48	80.5	0.395	18.80	86.2	0.199	3.397	90.7	0.272	0.604	96.5
M_2	0.027	10.15	91.6	0.277	15.71	95.8	0.115	2.318	98.4	0.104	0.223	99.7
M_3	0.022	10.00	85.5	0.202	14.78	89.6	0.073	2.137	92.9	0.050	0.371	97.5

meation. Acetone has lower viscosity but higher surface tension than hexane, and therefore has resulted in slow penetration through the hydrophobic membrane. Similarly, pentane has more flux due to its lower surface tension in spite of having higher viscosity. Similar observations were also reported by other researchers [51]. It can therefore be concluded that the permeability of solvent through hydrophobic membranes is dependent on the applied pressure, solvent viscosity and surface tension.

3. Identification of Competent Flux Decline Model

The reduction of permeate flux during the micro-filtration process was analyzed through various pore blocking models as discussed earlier. Fig. 14 illustrates the correlations of the models for all the three membranes corresponding to permeate flux data at a trans-membrane pressure of 137.89 kPa and oil concentration of 100 mg/L, 150 mg/L, 200 mg/L, and 250 mg/L. The correlation coefficient (R^2), slope and intercept for the all models are shown in Table 7. The correlation coefficients from the plots were evaluated to determine the most competent flux decline model with respect to the fouling phenomena. From the analysis, the cake filtration model with highest R^2 value (0.965-0.997) is found to best represent the experimental data. Similar observations has been reported in the micro-filtration of industrial oily wastewater using polymeric membranes [52] and kaolin based ceramic membranes [53] by other researchers.

CONCLUSION

Preparation and characterization of the low cost kaolin-based ceramic membranes (M_1, M_2 and M_3) were carried out in our earlier work [38]. Dead-end microfiltration was successfully carried out for separation of oil from stable oil-in-water emulsion with these membranes. All the membranes showed higher rejection at higher feed concentration and lower applied pressure. The maximum rejection was 95.4% for feed oil concentration of 250 mg/L and applied pressure of 137.89 kPa with M_1 membrane. However, flux permeation in M_1 membrane was less compared to that of M_2. The rejection in M_2 (93.6%) was also comparable to M_1 under identical feed concentration and applied pressure. Evaluation of the selection parameters indicates M_2 membrane as the highest performing membrane with SP value of 14.78×10^{-6} $m^3/m^2{\cdot}s$ and is recommended for industrial applications. The fouling model analysis shows that the cake filtration model best represents the experimental flux declination. Nonpolar solvents have higher permeability compared to the polar solvents, and the controlling factors for the membrane permeation were found to be the trans-membrane pressure, viscosity and the surface tension of the solvent. On the basis of the present experimentation, the competency of the prepared low cost ceramic membranes may be considered significant in the direction of useful application for treatment of industrial oily wastewater.

ACKNOWLEDGEMENTS

The authors sincerely acknowledge the Director, CSIR-NEIST for his permission to publish this work.

REFERENCES

1. A. Ezzati, E. Gorouhi and T. Mohammadi, *Desalination*, **185**, 371 (2005).
2. T. C. Arnot, R. W. Field and A. B. Koltuniewicz, *J. Membr. Sci.*, **169**, 1 (2000).
3. I. W. Cumming, R. G. Holdich and I. D. Smith, *J. Membr. Sci.*, **169**, 147 (2000).
4. T. Mohammadi, A. Pak, M. Karbassian and M. Golshan, *Desalination*, **168**, 201 (2004).
5. F. L. Hua, Y. F. Tsang, Y. J. Wang, S. Y. Chan, H. Chuand and H. N. Sin, *Chem. Eng. J.*, **128**, 169 (2007).
6. B. K. Nandi, R. Uppaluri and M. K. Purkait, *Sep. Sci. Technol.*, **44**, 2840 (2009).
7. B. Chakrabarty, A. K. Ghoshal and M. K. Purkait, *J. Membr. Sci.*, **325**, 427 (2008).
8. R. Mallada and M. Menendez, Inorganic Membranes: Synthesis, Characterization and Applications, Elsevier Science, Amsterdam, the Netherlands (2008).
9. L. J. Stack, P. A. Carney, H. B. Malone and T. K. Wessels, *Ultrason. Sonochem.*, **12**, 153 (2005).
10. P. Canizares, F. Martinez, C. Jimenez, C. Saez and M. A. Rodrigo, *J. Hazard. Mater.*, **151**, 44 (2008).
11. K. Bensadok, M. Belkacem and G. Nezzal, *Desalination*, **206**, 440 (2007).
12. F. L. Hua, Y. F. Tsang, Y. J. Wang, S. Y. Chan, H. Chuand and H. N. Sin, *Chem. Eng. J.*, **128**, 169 (2007).
13. J. Zhou, Q. Chang, Y. Wang, J. Wang and G. Meng, *Sep. Purif. Technol.*, **75**, 243 (2010).
14. W. Chen, J. Peng, Y. Su, L. Zheng, L. Wang and Z. Jiang, *Sep. Purif. Technol.*, **66**, 591 (2009).
15. Z. Ziaka and S. Vasileiadis, *Membrane Reactors for Fuel Cells and Environmental Energy Systems*, Indianapolis, Xlibris Publishing Co., U.S.A. (2009).
16. S. Vasileiadis, Z. Ziaka and M. Dova, *Int. J. Eng. Technol.*, **2**, 630 (2012).
17. Z. Ziaka and S. Vasileiadis, *J. Renew. Energy*, **2013**, 1 (2013).
18. S. Vasileiadis, Z. Ziaka, M. Tsimpa and E. Vasileiadou, *Global J.*

Inc., **12**, 19 (2012).
19. Z. Ziaka and S. Vasileiadis, *Sep. Sci. Technol*., **46**, 224 (2011).
20. S. Vasileiadis, Z. Ziaka and M. Tsimpa, *Int. Trans. J. Eng. Manage. Appl. Sci. Technol*., **2**, 129 (2011).
21. Z. Ziaka, A. Navrozidou, L. Paraschopoulou and S. Vasileiadis, *J. Nanosci. Nanotechnol*., **10**, 1 (2010).
22. S. Vasileiadis and Z. Ziaka, *J. Nano Res*., **12**, 105 (2010).
23. D. Bae, D. Cheong, K. Han and S. Choi, *Ceram. Int*., **24**, 25 (1998).
24. J. M. Benito, A. Conesa, F. Rubio and M. A. Rodriguez, *J. Eur. Ceram. Soc*., **25**, 1895 (2005).
25. G. Pugazhenthi, S. Sachan, N. Kishore and A. Kumar, *J. Membr. Sci*., **254**, 229 (2005).
26. X. Ding, Y. Fan and N. Xu, *J. Membr. Sci*., **270**, 179 (2006).
27. C. Falamaki, M. S. Afarani and A. Aghaie, *J. Eur. Ceram. Soc*., **24**, 2285 (2004).
28. K. A. DeFriend, M. R. Wiesner and A. R. Barron, *J. Membr. Sci*., **224**, 11 (2003).
29. W. Zeng, L. Goa, L. Gui and J. Guo, *Ceram. Int*., **25**, 723 (1999).
30. N. Saffaj, M. Persin, S. A. Younssi, A. Albizan, M. Bouhria, H. Loukili, H. Dacha and A. Larbot, *Sep. Purif. Technol*., **47**, 36 (2005).
31. N. Saffaj, M. Persin, S. A. Younsi, A. Albizane, M. Cretin and A. Larbot, *Appl. Clay Sci*., **31**, 110 (2006).
32. S. Khemakhem, A. Larbot and R. B. Amara, *Desalination*, **200**, 307 (2006).
33. M. R. Weir, E. Rutinduka, C. Detellier, C. Y. Feng, Q. Wang, T. Matsuura and R. Le Van Mao, *J. Membr. Sci*., **182**, 41 (2001).
34. K. Khider, D. E. Akretche and A. Larbot, *Desalination*, **167**, 147 (2004).
35. F. Bouzerara, A. Harabi, S. Achour and A. Larbot, *J. Eur. Ceram. Soc*., **26**, 1663 (2006).
36. M. Kazemimoghadam, A. Pak and T. Mohammadi, *Micropor. Mesopor. Mater*., **70**, 127 (2004).
37. A. Belouatek, N. Benderdouche, A. Addou, A. Ouagued and N. Bettahar, *Micropor. Mesopor. Mater*., **85**, 163 (2005).
38. B. Das, B. Chakrabarty and P. Barkakati, *Ceram. Int*., **42**, 14326 (2016).
39. J. Zhong, X. Sun and C. Wang, *Sep. Purif. Technol*., **32**, 93 (2003).
40. M. Ebrahimi, K. S. Ashaghi, L. Engel, D. Willershausen, P. Mund, P. Bolduan and P. Czermak, *Desalination*, **245**, 533 (2009).
41. A. Lobo, A. cambiella, J. M. Benito, C. Pazos and J. Coca, *J. Membr. Sci*., **278**, 328 (2006).
42. J. Cui, X. Zhang, H. Liu, S. Liu and K. L. Yeung, *J. Membr. Sci*., **325**, 420 (2008).
43. C. Yang, G. Zhang, N. Xu and J. Shi, *J. Membr. Sci*., **142**, 235 (1998).
44. S. R. H. Abadi, M. R. Sebzari, M. Hemati, F. Rekabdar and T. Mohammadi, *Desalination*, **265**, 222 (2011).
45. D. Vasanth, G. Pugazhenthi and R. Uppaluri, *J. Membr. Sci*., **379**, 154 (2011).
46. P. Monash and G. Pugazhenthi, *Desalination*, **279**, 104 (2011).
47. B. K. Nandi, A. Moparthi, R. Uppaluri and M. K. Purkait, *Chem. Eng. Res. Des*., **88**, 881 (2010).
48. J. Hermia, *Trans. Inst. Chem. Eng*., **60**, 183 (1982).
49. Y. Pan, W. Wang, T. Wang and P. Yao, *Sep. Purif. Technol*., **57**, 388 (2007).
50. B. Chakrabarty, A. K. Ghoshal and M. K. Purkait, *J. Membr. Sci*., **309**(1-2), 209 (2008).
51. D. Bhanushali, S. Kloos, C. Kurth and D. Bhattacharyya, *J. Membr. Sci*., **189**, 1 (2001).
52. A. Salahi, A. Gheshlaghi, T. Mohammadi and S. S. Madaeni, *Desalination*, **262**, 235 (2010).
53. D. Vasanth, G. Pugazhenthi and R. Uppaluri, *Desalination*, **320**, 86 (2013).